FINITE ELEMENT ANALYSES OF TOE-GROUND WELDED CRUCIFORM -JOINTS SUBJECTED TO LOW-CYCLE FATIGUE CONDITIONS.

T.L. Dickerson*

Finite element models have been developed to predict the local straining behaviour in weld toes of fatigue test specimens that have been burr-ground. The models have been validated against experimental load and displacement behaviour and shown to be independent of the loading gauge length. For low cycle fatigue it has also shown is that the local strain is more appropriate for predicting life than a strain or stress remote from the weld toe. Relating these strains to crack initiation life via a strain-life law gave good agreement with experimental initiation lives; however, some inconsistencies were apparent.

INTRODUCTION

Fatigue life improvement of structures can be gained by reducing the difference between the fatigue performance of welds and the parent material, this usually involves dressing of the weld toes. Among others, Gurney (1) and Haagensen (2) clearly show that techniques such as toe burr-grinding or TIG-dressing are particularly beneficial in the low stress (strain) regime. Harrison (3) and Watkinson et al (4) demonstrated a reduction in benefit at high strains using high strength steels; however, because high strength steels were used the plastic strains were limited. The fatigue data (3,4) enabled weld improvement techniques to be included in the British Standard pressure vessel design code, BS5500 (5). This is one of thre few national or international design code that explicitly allows the use of improvement techniques, hence there is great potential for allowing either an extension of design life, or increased cyclic loading levels.

Recently, Dickerson (6,7) reported on experimental work to determine the life extension benefit of weld improvement in the low cycle fatigue regime. Cruciform specimens were cycled under load or displacement (nominal strain) control. Lower strength steel was used than in the previous studies (3,4), hence the plastic strains were much greater in this work. The work showed shorter lives with burr-ground weld toes than obtained from untreated welds, although only at high strains and where substantial cross-section was lost. This study investigated the straining of the burr-ground

* TWI, Abington Hall, Abington, Cambridgeshire, CB1 6AL, UK

cruciform test specimens, used in the above mentioned tests, by using elastic-plastic finite element analyses.

MODELLING APPROACH

The geometry of the test specimens is shown in Fig.1; the gauge length, G=100mm, was the distance over which the nominal strain were controlled using extensometers. The sinusoidally applied cyclic extensions were from zero up to a maximum of dG=0.27mm, see Fig.1.

The ABAQUS general purpose finite element program was used for the modelling. The specimens were nominally symmetrical on two planes, hence ¼-symmetric 2D meshes were constructed. The elements used were 8-noded generalised plane strain with reduced integration (element CPE8R). A typical mesh is shown in Fig.2, along with an indication of the boundary conditions. The cyclic stress-strain material behaviour for the parent material was determined by Branco (8); this was used as a basis for the material property definition in the models. Because of an ABAQUS limitation, a bi-linear stress-strain approximation had to be defined for the cyclic plasticity stress-strain law. The full and bi-linear curves are shown in Fig.3; kinematic hardening was used. Loading was applied between zero and dG/2 (because of symmetry) using defined displacements along A-A in Fig.2.

MODEL VALIDATION

Two cyclic load-displacement curves, for two values of dG, are shown in Fig.4 along with experimental load measurements; Fig.5 shows the total load ranges. Initially the models' total loads were about 10% lower than found experimentally, the discrepancy being less for lower dG. This indicates that a combined kinematic/isotropic rule may have been more appropriate. To compensate, the stress-strain curve was modified, as shown in Fig.3, by increasing the stress. Generally, good agreement can be seen in Fig.5 for the actual and predicted loads. However, as the analysis is based on strains and the loading is displacement controlled the errors introduced by the changes to the stress-strain behaviour will be minimal.

GAUGE LENGTH

The cruciform and the welds will stiffen the central part of the specimen producing a non-uniform strain distribution along the specimen. A relatively large welded region may mean the nominal strain is unrepresentative of the strains in components where the effective gauge length may be different.

Increasing the model length gave results that were asymptotic, 500mm gauge length models gave results that had converged. Figure 6 shows strain distributions

along the surface of as-welded and burr-ground models for two gauge lengths. Although the as-welded models show that the 100mm model has a remote axial strain about 25% greater than the nominal strain and the 500mm model, the local strain at the weld toe is similar (identical meshes at the weld toe). Experimental results show (7) that with a gauge length of 100mm failure lives are consistent with load controlled tests. Figure 6 also shows no significant difference between burr-groove strains for the different length models. The models and the experiments confirm that a 100mm gauge length will give results that are effectively independent of the gauge length. They also indicate that the local strain is the important factor and that analyses using nominal strains may be of limited use.

LIFE PREDICTION OF BURR-GROUND JOINTS

Branco (8) carried out strain-cycled fatigue tests on the material used to make the specimens, a Morrow strain-life equation was developed:-

$$\frac{\Delta\varepsilon_T}{2} = \frac{\Delta\varepsilon_e}{2} + \frac{\Delta\varepsilon_p}{2} = \frac{727}{E}(2\cdot N_i)^{-0.09} + 0.36(2\cdot N_i)^{-0.56}$$

This was used to determine the life to crack initiation (N_i) from the local total-strain range ($\Delta\varepsilon_T$) in the burr groove, $\Delta\varepsilon_T$ was obtained from the FEA models. The results from the analyses are plotted on a strain-life curve in Fig.7; the strain is expressed in terms of the pseudo-elastic stress ($E\cdot\Delta\varepsilon_T$) and the life is to crack initiation in cycles. Also shown in Fig.7 are experimental data for the life to initiation for joints burr-ground with either a R=3mm or 8mm burr and life predictions for both burr sizes.

In Fig.7 it can be seen that the slopes of the predicted life curves are similar to the slope of the experimental results. The curves for the two burr radii specimens are converging as the strain is increased; this was a feature of experimental data (7). However, the life predictions for the specimens with the 3mm and the 8mm grooves show a substantial difference whereas the experimental results showed a much smaller difference between the two (7), particularly at high strains.

STRAIN CONCENTRATION FACTORS

Figures 8 and 9 show details of strain concentrations (SC) for a range of practical joint sizes, burr sizes and groove depths; the figures pertain to cruciform specimens with t=T. For convenience, the specimen dimensions have been normalised with respect to the parent material thickness. The strain concentration factors were defined as:-

$$SC_{elastic} = \frac{\Delta\varepsilon_e}{(\sigma_{nom} \div E)} \qquad SC_{elastic\_plastic} = \frac{\Delta\varepsilon_T}{\varepsilon_{nom}}$$

Where $\Delta\varepsilon_e$ were determined from load controlled elastic analyses and $\Delta\varepsilon_T$ is the total strain determined from the full cyclic elastic-plastic analyses. σ_{nom} is the nominal axial stress on a section remote from the joint and $\varepsilon_{nom} = dG/G$.

DISCUSSION

The straining behaviour of the specimens is illustrated in Fig.2, which shows contours of the axial total-strain. A narrow band of increased yielding can be seen; it starts in the burr groove and extends at 45° to the direction of the load. This yield band is caused by the reduction of the area of the specimen due to burr grinding. In the groove the strain will also be affected by the groove geometry and its position relative to the weld. It has been demonstrated that FEA can be used to determine the global stress and strain behaviour of the specimens.

The ability to predict the local strains in the burr groove adequately is less certain. Crack initiation life predictions were made and compared to experimental data. The actual lives were under-predicted (see Fig.7) by as much as an order of magnitude for R=3mm, but the R=8mm predictions gave much better results. However, a relatively simple life prediction model was used; for instance mean stress effects were ignored. The predictions for specimens with different groove radii gave considerably different life predictions whereas the experimental investigation (6,7) showed much less of a difference. The reason for inconsistency is not known and further work is needed to resolve it.

Figure 8 shows how the total strain varies with geometric parameters. As the figure clearly shows, decreasing the (relative) burr groove radius increases the strain concentration. For very small values of R/T, which in practice pertain to thick sections, the strain concentration can be very high. As the relative radius of a burr will get smaller as the section thickness increases, then a thickness-effect for burr ground welds is predicted. Also for larger joint thickness the relative depth of groove will reduce, this is a competing effect to that caused by the relative radius but it is clear from the figure that the radius change has the dominant effect on the SC for all but very small relative radii. Further work will be needed to determine if this thickness effect is more or less severe than the penelty imposed by design codes (e.g. 5) due to plate thickness.

The predicted behaviour is inconsistent with experimental data which showed little effect of burr radius at high strain ranges and the loss of benefit of improvement was attributed to loss of load bearing section at the burr grooves (7).

REFERENCES

(1) Gurney, T.R., "Fatigue of Welded Structures", 2nd Edition, Cambridge University Press, Cambridge , England, UK, 1979.

Delft University Press, 1989.

(3) Harrison, J.D., "Techniques for improving the fatigue strength of welded high strength steels", Welding Institute Report No. C215/7/68, 1968.

(4) Watkinson, F., Bodger, P.H. and Harrison J.D., "The fatigue strength of welded joints in high strength steels and methods for its improvement", Welding Institute Report No. C215/16/70, 1970.

(5) BS5500:1994, "British Standard Specification for Unfired Fusion Welded Pressure Vessels: Enquiry case 79", BSI, London, 1994.

(6) Dickerson, T.L., "Weld Improvement Methods for low Cycle Fatigue Applications", TWI Report Number 88159/7/95 for the ECSC (contract No. 7210-MC/801), TWI, Cambridge, England, UK, 1995.

(7) Dickerson, T.L., "Low-cycle Fatigue of Welded Cruciform Joints with Fatigue Life Improvement Applied to the Weld Toes", Int. Conf. on Fatigue of Welded Components and Structures, Paris, France, 12-14 June 1996.

(8) Branco, C.M., "Weld Improvement Methods for low Cycle Fatigue Applications", CEMUL report for the ECSC (contract No. 7210-MC/931), Lisbon, Portugal, 1995.

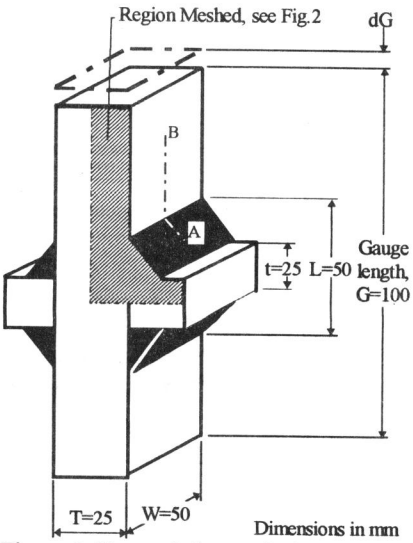

Figure 1 Size and shape of the test joint modelled (Toe grooves not shown)

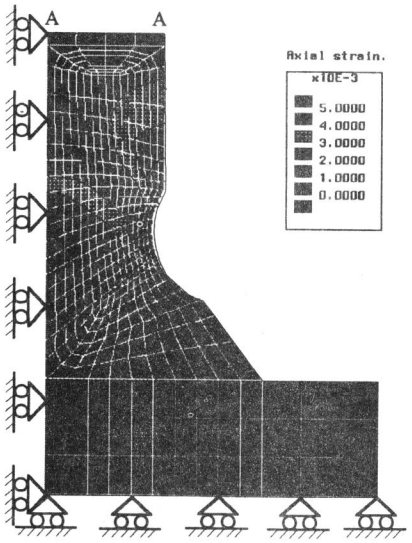

Figure 2 A typical finite element mesh showing symmetry boundary conditions and contours of total axial strain.

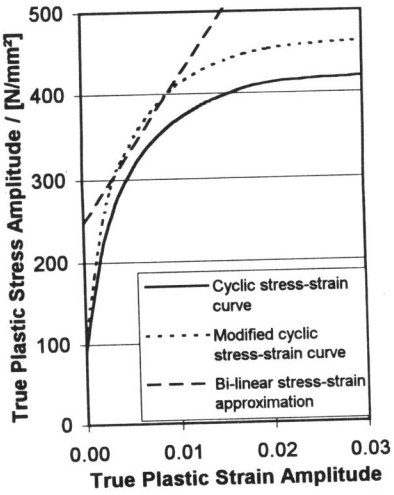

Figure 3. The cyclic stress-strain behaviour used in the models.

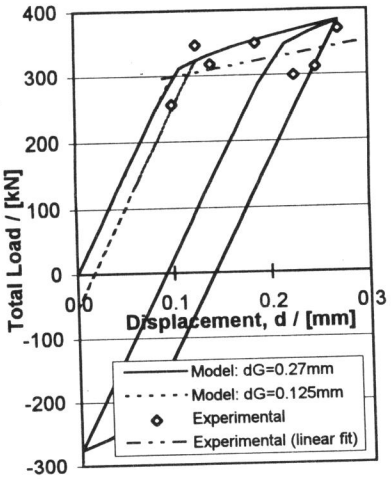

Figure 4. The models' load-displacement curves and experimental results for as-welded specimens.

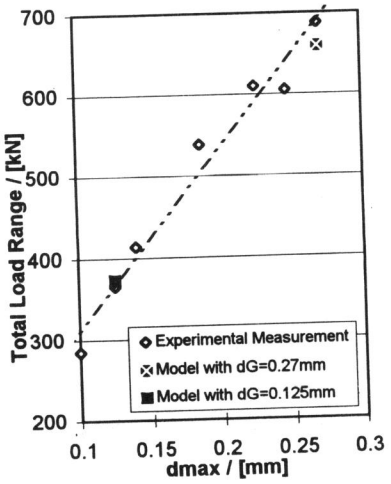

Figure 5. Cyclic load range verses maximum displacement for as-welded joints.

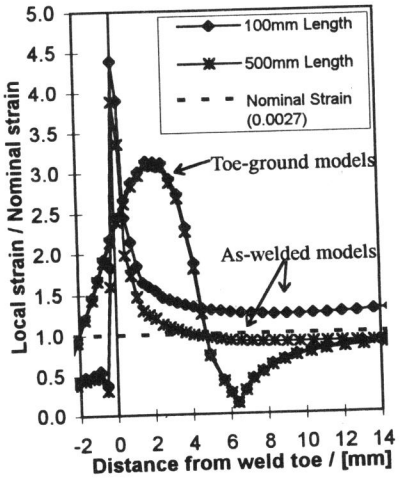

Figure 6. Surface strain distributions along the loaded members of cruciform joint models (between A and B in Fig.1.)

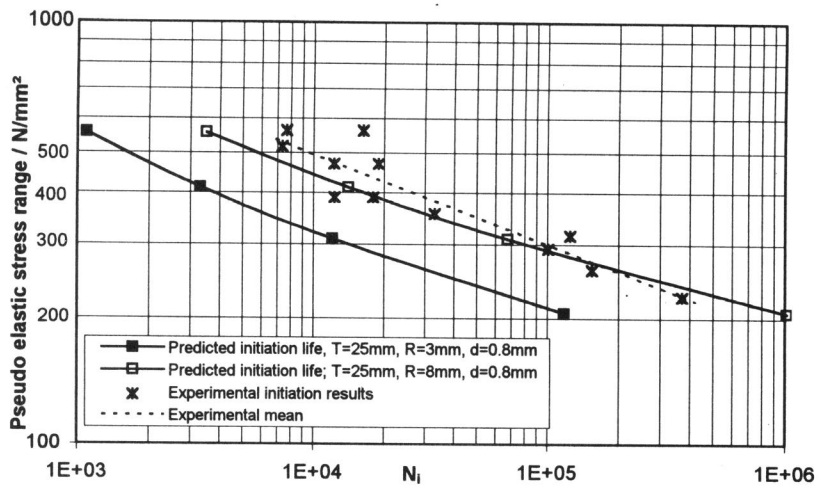

Figure 7. Plot of the pseudo elastic stress range (nominal) verses actual experimental and predicted lives of burr-ground cruciform test specimens.

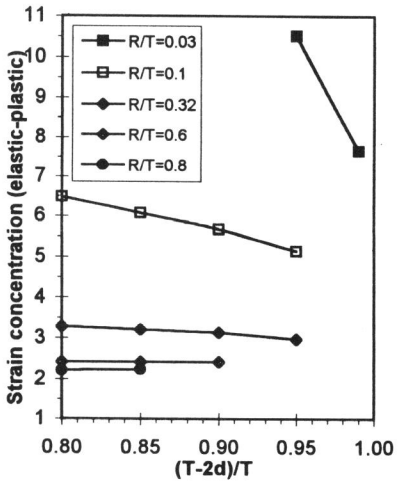

Figure 8. Change of strain concentration with geometric parameters. Nominal axial strain, ε_{nom}=0.0027.

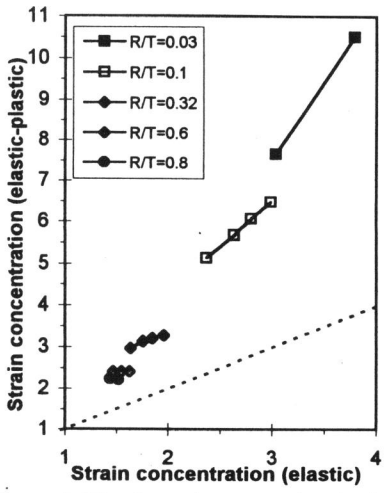

Figure 9. Elastic strain verses the elastic-plastic strain in the burr grooves. ε_{nom}=0.0027.